

Secure Pinching Antenna-aided ISAC

Elmehdi Illi, *Member, IEEE*, Marwa Qaraqe, *Senior Member, IEEE*, and Ali Ghrayeb, *Fellow, IEEE*

Abstract—In this letter, a pinching antenna (PA)-aided scheme for establishing a secure integrated sensing and communication system (ISAC) is investigated. The underlying system comprises a dual-functional radar communication (DFRC) base station (BS) linked to multiple waveguides to serve several downlink users while sensing a set of malicious targets in a given area. The PA-aided BS aims at preserving communication confidentiality with the legitimate users while being able to detect malicious targets. One objective of the proposed scheme is to optimize the PA locations, based on which an optimal design of the legitimate signal beamforming and artificial noise covariance matrices is provided to maximize the network's sensing performance, subject to secrecy and total power constraints. We demonstrate the efficacy of the proposed scheme through numerical examples and compare that against a traditional DFRC ISAC system with a uniform linear array of half-wavelength-spaced antennas. We show that the proposed scheme outperforms the baseline PA-aided scheme with equidistant PAs by 3 dB in terms of illumination power, while it can provide gains of up to 30 dB of the same metric against a traditional ISAC system with half-wavelength-space uniform linear arrays.

Index Terms—Eavesdropping, integrated sensing and communication, physical-layer security, and pinching antennas.

I. INTRODUCTION

Integrated sensing and communication (ISAC) has emerged in the past few years as a means of supporting power- and spectrum-efficient sensing applications by utilizing the same hardware, frequency, and power resources for both sensing and communication tasks [1]. As well, the multiple-input multiple-output (MIMO) technology has been forming a key pillar in the fifth generation of cellular networks (5G), due to its great potential in enabling received signal strength enhancement and spatial multiplexing [2]. MIMO demonstrated notable gains in establishing robust communications, sensing, and ISAC schemes [1]. Nevertheless, MIMO can hardly turn an unfavorable channel to an advantageous one. To this end, movable antenna systems (MAS) and reconfigurable intelligent surfaces (RIS) techniques have been proposed as supportive techniques to MIMO. While MAS is based on adjusting antenna positions by few wavelengths, RIS is based on manipulating signal reflections through optimized phase shifts of its reflective elements. However, due to antenna position's tunability over only a few wavelengths, FAS fails in solving one of the MIMO main issues, that is, the line-of-sight (LoS) path blockage, while RIS suffers from the double path-loss, especially at higher frequencies.

A promising alternative, referred to as pinching-antenna systems (PASS), has been recently introduced by NTT DO-COMO [3]. PASS uses low-loss long dielectric waveguides to guide signals and radiate them through small dielectric elements, also known as pinching antennas (PAs) manually placed along the waveguide in positions of interest. This

setup exhibits several benefits compared to traditional MIMO, FAS, and RIS in overcoming LoS blockages and high free-space path loss (FSPL) in mmWave- and THz-band transmissions, and broadening network coverage in indoor and outdoor scenarios, thanks to its flexible antenna placement. Such a propagation-tuning feature makes PASS well suited for establishing physical layer security (PLS), where beamforming can be optimized to strengthen communication with legitimate users while weakening it with eavesdroppers.

The past year witnessed a notable growth in the number of works that designed and analyzed PASS in various setups. For instance, [4] analyzed the ergodic capacity of PASS. The work in [5]–[8] proposed an optimization framework for PASS by optimizing transmit PA locations, beamforming vector, and uplink transmit power to either maximize (minimize) the sum rate (transmit power) subject to power (sum rate) constraints. The authors of [9] maximized the network secrecy capacity (SC) with the use of an optimized artificial noise (AN), transmit beamforming, and PA positions. In [10]–[12], the authors analyzed the sensing and reliability performance of PA-aided ISAC systems (PA-ISACS), showing the potential of PASS to establish robust sensing and reliable communication in various scenarios.

Despite the aforementioned contributions, most of them were limited to maximizing the network reliability in terms of its achievable rate, sum rate, or secrecy rate. Furthermore, the work in [10]–[12] focused on PA-ISACS analysis and/or optimization only from the perspective of sensing and communication reliability, while missing the inclusion of the security aspect. Motivated by the above, this work aims to analyze and optimize the secrecy and sensing performance of a secure PA-ISACS. Using a suboptimal designed PA positions optimization scheme, along with semi-definite programming for optimal beamforming and AN covariance, a robust optimization framework is proposed to maximize the per-target sensing illumination power, subject to secrecy and total power constraints. The proposed scheme exhibits at least 3- and 30-dB gains in terms of sensing illumination power against a baseline PA-ISACS with equispaced PAs and against an ISAC system with a uniform linear array (ULA) of half-wavelength-spaced antennas, respectively.

II. SYSTEM MODEL

A. Signal and Channel Model

Consider a PA-ISACS system, as given in Fig. 1, comprising a base station (BS), labeled B , communicating with a set of G users $\{U_g\}_{g=1}^G$. Furthermore, a set of K malicious targets $\{T_k\}_{k=1}^K$ are present, where B , acting as an ISAC transceiver aims at sensing and detecting their presence in the pre-known locations. Furthermore, $\{T_k\}_{k=1}^K$ aim to compromise transmission by eavesdropping on legitimate signals of the G users. B is connected to N parallel dielectric waveguides through flexible cables. It is assumed that the n th waveguide

The authors are with the College of Science and Engineering, Hamad Bin Khalifa University, Qatar Foundation, Doha, Qatar. (e-mails: {eilli, mqaraqe, aghrayeb}@hbku.edu.qa).

is deployed in parallel to the x axis and at given y and z coordinates, denoted by y_n and z_n . To this end, M_t transmit PAs and M_r receive ones can be activated along each waveguide to enhance (i) the transmission channel to the set of users and targets and (ii) echo signals reception from the K targets. We denote by $(x_{n,m}, y_{n,m}, z_{n,m})$ the Cartesian coordinates of the m th transmit PA on the n th waveguide. Notably, due to the deployment of the parallel waveguides along the x axis, it yields $y_{n,m} = y_n$ and $z_{n,m} = z_n \forall m = 1, \dots, M_t$. In addition, the coordinates for each user U_g and target T_k are denoted as $(x_{U_g}, y_{U_g}, z_{U_g})$ and $(x_{T_k}, y_{T_k}, z_{T_k})$, respectively. The received signal at U_g and T_k can be expressed as [4]

$$\mathbf{y}_\Lambda = \mathbf{g}_{B\Lambda}(\mathbf{x}, \mathbf{y}, \mathbf{z}) \mathbf{H}(\mathbf{x}) \mathbf{s} + \mathbf{w}_\Lambda, \Lambda \in \{U_g, T_k\} \quad (1)$$

where $\mathbf{g}_{B\Lambda}(\mathbf{x}) \triangleq [\mathbf{g}_{B_1\Lambda}(\mathbf{x}_1, y_1, z_1), \dots, \mathbf{g}_{B_N\Lambda}(\mathbf{x}_N, y_N, z_N)] \in \mathbb{C}^{1 \times M_t N}$ is the channel response of the link between all the network's PAs and node Λ , and

$$\mathbf{g}_{B_n\Lambda}(\mathbf{x}_n, y_n, z_n) = \begin{bmatrix} \sqrt{\zeta_{B_{n,1}\Lambda}} e^{-j2\pi/\lambda d_{B_{n,1}\Lambda}}, \dots, \sqrt{\zeta_{B_{n,M_t}\Lambda}} e^{-j2\pi/\lambda d_{B_{n,M_t}\Lambda}} \end{bmatrix} \in \mathbb{C}^{1 \times M_t} \quad (2)$$

represents the channel response vector between the n th waveguide and node Λ . Additionally,

$$\zeta_{B_{n,m}\Lambda} = G^{(B_{n,m})} G^{(\Lambda)} \left(\frac{\lambda}{4\pi d_{B_{n,m}\Lambda}} \right)^2 \quad (3)$$

denotes the FSPL term between the m th antenna of the n th waveguide, labeled $B_{n,m}$, and Λ , and $G^{(B_{n,m})}$ is the transmit gain of $B_{n,m}$. Also, $G^{(\Lambda)}$ is node Λ 's receive antenna gain, λ is the signal wavelength, and

$$d_{B_{n,m}\Lambda} = \sqrt{(x_{n,m} - x_\Lambda)^2 + (y_n - y_\Lambda)^2 + (z_n - z_\Lambda)^2} \quad (4)$$

is the distance between $B_{n,m}$ and node Λ . Also, $\mathbf{x}_n = [x_{n,1}, \dots, x_{n,M_t}]$ denotes the position vector for the M_t antennas of the n th waveguide along the x -axis with $\mathbf{x} \triangleq [\mathbf{x}_1, \dots, \mathbf{x}_N]$, while $\mathbf{y} \triangleq [y_1, \dots, y_N]$ and $\mathbf{z} \triangleq [z_1, \dots, z_N]$ are the waveguides positions along the y and z axes, respectively.

Remark 1. By assuming that the waveguides are deployed over fixed y_n and z_n values, the channel vectors' dependence on y_n and z_n will be omitted in the sequel and the considered PA-ISACS performance evaluation and optimization will be performed with respect to the PA positions over the x -axis.

On the other hand, we define

$$\mathbf{H}(\mathbf{x}) \triangleq \begin{bmatrix} \mathbf{h}(\mathbf{x}_1) & \mathbf{0}_{M_t \times 1} & \dots & \mathbf{0}_{M_t \times 1} \\ \mathbf{0}_{M_t \times 1} & \mathbf{h}(\mathbf{x}_2) & \dots & \mathbf{0}_{M_t \times 1} \\ \vdots & \vdots & \ddots & \vdots \\ \mathbf{0}_{M_t \times 1} & \mathbf{0}_{M_t \times 1} & \dots & \mathbf{h}(\mathbf{x}_N) \end{bmatrix} \in \mathbb{C}^{NM_t \times N} \quad (5)$$

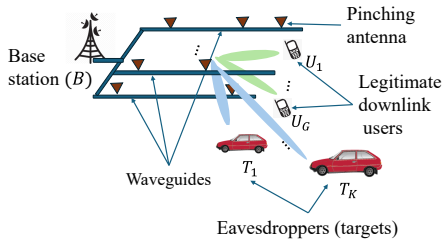


Fig. 1: Considered pinching-antenna-enabled ISAC system.

as the overall in-waveguide channel matrix for the N waveguides with $\mathbf{0}_{M_t \times 1}$ being an all-zeros column vector of M_t elements, and

$$\mathbf{h}(\mathbf{x}_n) = \begin{bmatrix} \sqrt{\theta_{n,1}} e^{-j2\pi/\lambda n_g x_{n,1}}, \dots, \sqrt{\theta_{n,M_t}} e^{-j2\pi/\lambda n_g x_{n,M_t}} \end{bmatrix}^T \in \mathbb{C}^{M_t \times 1} \quad (6)$$

as the in-waveguide propagation vector for the n th waveguide, which represents the signal attenuation from B to $B_{n,m}$, and $\theta_{n,m}$ is the ratio of signal power radiated by $B_{n,m}$. Note from (1) that each waveguide's antennas radiate the same signal, increasing the transmit power level. Without loss of generality, an equal-power model is considered as utilized in [4, Eqs. (20), (21)], i.e., $\theta_{n,m} = \theta, \forall n, m$, where $0 < \theta \leq 1/M_t$. Also, n_g defines the refractive index of the waveguide medium, and $\mathbf{s} = \mathbf{V}\mathbf{u} + \mathbf{w} \in \mathbb{C}^{N \times 1}$ is the signal vector containing the N transmit signals by the N waveguides. Furthermore, $\mathbf{V} = [\mathbf{v}_1, \dots, \mathbf{v}_G] \in \mathbb{C}^{N \times G}$ is the pinching beamforming matrix used to beamsteer the G users' signals simultaneously by the PASS composed of $M_t N$ radiating antennas, where $\mathbf{v}_g \in \mathbb{C}^{N \times 1}$ denotes U_g 's beamforming vector, and $\mathbf{u} = [u_1, \dots, u_G] \in \mathbb{C}^{G \times 1}$ is the raw data signal vector of the G users. On the other hand, the system beamforms an AN signal $\mathbf{w} \in \mathbb{C}^{N \times 1}$ with the objective of (i) degrading the decoding performance at the malicious targets and increase the degrees of freedom in sensing their presence. \mathbf{w} is considered as a zero-mean complex Gaussian vector with covariance matrix $\mathbf{W} = \mathbb{E}[\mathbf{w}\mathbf{w}^H]$, where $(\cdot)^H$ denotes the Hermitian of a vector/matrix and $\mathbb{E}[\cdot]$ is the expectation operator. Both the legitimate signal and AN beamforming are subject to a total power budget constraint, i.e., $\sum_{g=1}^G \text{Tr}[\mathbf{V}_g] + \text{Tr}[\mathbf{W}] \leq P_{\max}$, where $\mathbf{V}_g \triangleq \mathbf{v}_g \mathbf{v}_g^H$, P_{\max} is the system power budget, and $\text{Tr}[\cdot]$ is the trace of a matrix. Lastly, \mathbf{w}_Λ is the zero-mean additive white Gaussian noise (AWGN) at node Λ of variance σ_Λ^2 . Per the received signal formula in (1), and exploiting the properties of positive semidefinite (PSD) matrices, the received signal-to-interference-and-noise ratio (SINR) at U_g and T_k to decode u_g can be expressed as

$$\gamma_\Lambda^{(g)}(\{\mathbf{V}_g\}_{g=1}^G, \mathbf{W}, \mathbf{x}) = \frac{\text{Tr}(\mathbf{F}_{B\Lambda}(\mathbf{x}) \mathbf{V}_g)}{\text{Tr}\left(\mathbf{F}_{B\Lambda}(\mathbf{x}) \left[\mathbf{W} + \sum_{\substack{g'=1 \\ g' \neq g}}^G \mathbf{V}_{g'}\right]\right) + \sigma_\Lambda^2}, \quad (7)$$

where $\mathbf{F}_{BT_k}(\mathbf{x}) \triangleq \mathbf{f}_{B\Lambda}^H(\mathbf{x}) \mathbf{f}_{B\Lambda}(\mathbf{x})$ and $\mathbf{f}_{B\Lambda}(\mathbf{x}) \triangleq \mathbf{g}_{B\Lambda}(\mathbf{x}) \mathbf{H}(\mathbf{x})$.

B. Secrecy Performance Metrics

The secrecy capacity is the performance metric we adopt in this paper to evaluate the performance of the overall system, which can be formulated for securely decoding u_g in the presence of T_k as

$$C_s^{(g,k)}(\{\mathbf{V}_g\}_{g=1}^G, \mathbf{W}, \mathbf{x}) = \left[\begin{array}{c} C_{U_g}^{(g)}(\{\mathbf{V}_g\}_{g=1}^G, \mathbf{W}, \mathbf{x}) \\ -C_{T_k}^{(g)}(\{\mathbf{V}_g\}_{g=1}^G, \mathbf{W}, \mathbf{x}) \end{array} \right]^+, \quad (8)$$

where $[t]^+ \triangleq \max(0, t)$, while

$$C_\Lambda^{(g)}(\{\mathbf{V}_g\}_{g=1}^G, \mathbf{W}, \mathbf{x}) = \log_2 \left(1 + \gamma_\Lambda^{(g)}(\{\mathbf{V}_g\}_{g=1}^G, \mathbf{W}, \mathbf{x}) \right) \quad (9)$$

is the channel capacity of the link to node Λ , computed using (7). Due to the consideration of multiple legitimate users and malicious eavesdroppers, the equivalent system's SC is defined as the worst-case SC, i.e.,

$$C_s \left(\{\mathbf{V}_g\}_{g=1}^G, \mathbf{W}, \mathbf{x} \right) = \min_{\substack{g=1, \dots, G \\ k=1, \dots, K}} C_s^{(g,k)} \left(\{\mathbf{V}_g\}_{g=1}^G, \mathbf{W}, \mathbf{x} \right). \quad (10)$$

C. Sensing Performance Metrics

The considered system desires ensuring monostatic radar sensing to detect the presence of the K malicious targets. By virtue of the flexible channel response adjustment through PA location fine-tuning, the ISAC transceiver aims at establishing a robust beamsteering through the set of waveguides and antennas to illuminate the K targets with a maximal electromagnetic power. The higher the latter, the greater the echo signal reflected back to the ISAC receiver, maximizing the target detection probability. Thus, the sensing performance is quantified by the illumination power, defined as

$$Q_s^{(k)}(\mathbf{R}_s, \mathbf{x}) = \sigma_{RCS}^{(k)} 4\pi \text{Tr} [\mathbf{F}_{BT_k}(\mathbf{x}) \mathbf{R}_s] / G^{(T_k)}, \quad (11)$$

where $\mathbf{R}_s \triangleq \sum_{g=1}^G \mathbf{V}_g + \mathbf{W}$. In (11), $Q_s^{(k)}(\mathbf{R}_s, \mathbf{x})$ indicates the level of electromagnetic power illuminating T_k , where $\sigma_{RCS}^{(k)}$ is the radar cross section (RCS) of T_k .

Another metric for evaluating the sensing performance is the illumination power pattern, expressed as

$$Q_s(\mathbf{R}_s, \mathbf{x}, x_0, y_0, z_0) = \bar{\sigma}_{RCS} 4\pi \text{Tr} [\mathbf{F}_0(\mathbf{x}, x_0, y_0, z_0) \mathbf{R}_s], \quad (12)$$

where $\mathbf{F}_0(\mathbf{x}, x_0, y_0, z_0) \triangleq \mathbf{f}_0^H(\mathbf{x}, x_0, y_0, z_0) \mathbf{f}_0(\mathbf{x}, x_0, y_0, z_0)$, $\mathbf{f}_0(\mathbf{x}, x_0, y_0, z_0) = \mathbf{g}_0(\mathbf{x}, x_0, y_0, z_0) \mathbf{H}(\mathbf{x})$, with $\mathbf{g}_0(\mathbf{x}, x_0, y_0, z_0)$ can be computed from (2) and (6) by setting $G^{(\Lambda)} = 1$ in the FSPL term, computed using (3), while the distance $d_{B_{n,m}\Lambda}$ is substituted by $d_{B_{n,m},P_0}$, evaluated from (4) by substituting $(x_\Lambda, y_\Lambda, z_\Lambda)$ by (x_0, y_0, z_0) . Also, $\bar{\sigma}_{RCS}$ is the average RCS across the K targets. Note that $Q_s(\mathbf{R}_s, \mathbf{x}, x_0, y_0, z_0)$ is similar to the sensing beampattern metric, measuring the transmit signal power's angular directivity over the BS's angular look direction, while $Q_s(\mathbf{R}_s, \mathbf{x}, x_0, y_0, z_0)$ assesses the transmit power illumination level at each point $P_0(x_0, y_0, z_0)$ served by the array of PAs, which effectively evaluates the level of power reaching the locations of interest, i.e., targets' locations.

III. SECURE PA-ISAC OPTIMIZATION

A. Optimization Problem Formulation

The optimization problem under consideration aims at maximizing the sensing performance, subject to secrecy constraints. The PA-ISAC system utilizes pinching beamforming by leveraging the set of PAs of the various waveguides. The set of PAs offers flexibility in adjusting the wireless and in-waveguide channel response, i.e., (2) and (6), whereas the beamforming and AN covariance matrices can further enhance signal beamsteering. In the considered design, the sensing performance is prioritized. Thus, the optimization framework consists of optimizing the PA locations, the transmit signal beamforming and AN covariance matrices in order to maximize the sensing

illumination power per target, subject to total power and secrecy constraints. This is formulated as

$$\mathcal{P}1: \max_{\{\mathbf{V}_g\}_{g=1}^G, \mathbf{W}, \mathbf{x}} \min_{k=1, \dots, K} Q_s^{(k)}(\mathbf{R}_s, \mathbf{x}) \quad (13a)$$

$$\text{s.t. (C1): } C_s \left(\{\mathbf{V}_g\}_{g=1}^G, \mathbf{W}, \mathbf{x} \right) \geq C_{s,lb} \quad (13b)$$

$$\text{(C2): } \text{rank}(\mathbf{V}_g) = 1, \forall g \quad (13c)$$

$$\text{(C3): } \mathbf{V}_g \geq \mathbf{0}, \forall g, \mathbf{W} \geq \mathbf{0} \quad (13d)$$

$$\text{(C4): } \sum_{g=1}^G \text{Tr}[\mathbf{V}_g] + \text{Tr}[\mathbf{W}] \leq P_{\max} \quad (13e)$$

$$\text{(C5): } x_{n,m} - x_{n,m-1} \geq \Delta x, \forall n, \forall m \geq 2 \quad (13f)$$

$$\text{(C6): } x_{n,m} \geq x_0, x_{n,m} \leq x_{\max} \quad (13g)$$

where (C1) is the minimal secrecy requirement constraint with $C_{s,lb}$ representing the minimal network's SC requirement, while (C2) and (C3) define the rank-one property of $\{\mathbf{V}_g\}_{g=1}^G$ and the positive semidefiniteness property of the latter and \mathbf{W} , where $\mathbf{A} \geq \mathbf{0}$ denotes that \mathbf{A} is a PSD matrix. (C4) defines the total power budget constraint, and (C5)-(C6) refer to the constraints on each PA's location, where Δx is the minimal inter-PA separation, whereas x_0 and x_{\max} define the interval for each PA's position. $\mathcal{P}1$ is challenging to handle due to the coupling between the PAs locations-dependent channel matrix $\mathbf{F}_{B\Lambda}(\mathbf{x})$ and $\{\mathbf{V}_g\}_{g=1}^G, \mathbf{W}$, as noted from (7) and (11). Also, for given $\{\mathbf{V}_g\}_{g=1}^G, \mathbf{W}$, another hurdle to optimize \mathbf{x} is the non-convexity of $Q_s^{(k)}(\{\mathbf{V}_g\}_{g=1}^G, \mathbf{W}, \mathbf{x})$ and $C_s(\{\mathbf{V}_g\}_{g=1}^G, \mathbf{W}, \mathbf{x})$ in \mathbf{x} , as noted from (7) and (11). This is caused essentially by the involvement of \mathbf{x} 's elements $(x_{n,m})$ in the complex exponentials in (2) via the distances $d_{B_{n,m}U_g}, d_{B_{n,m}T_k}(\forall g, k)$ and also in (6). It is worth mentioning that previous work aimed to solve similar problems in PASS using alternating optimization, such as in [5], [12], in which \mathbf{x} was optimized over two steps, by first solving for a slack channel matrix \mathbf{Z} maximizing the sensing or reliability performance, followed by performing an iterative element-wise line search to sequentially optimize (i.e., one PA location at once) the PAs locations producing the nearest channel response to \mathbf{Z} . Nonetheless, the schemes in [5], [12] did not consider secrecy constraints and the one in [12] was limited to a single user/target case. In addition, note that the line search-based solution for \mathbf{x} in the above work may produce a solution violating the constraints of $\mathcal{P}1$. Motivated by this, a novel algorithm for optimizing the PA locations is presented in the sequel.

B. PA Positions Optimization

The proposed PA positions optimization scheme is based on positioning the set of PAs in each waveguide closer to the users and targets to maximize their respective channel gains. Without loss of generality, it is assumed that $M_t > G$ and $M_t > K$. For each waveguide, the proposed approach starts by placing the first G PAs aligned with the G users, i.e., $x_{n,g} = x_{U_g}, g = 1, \dots, G, \forall n$. Then, the set of targets are evaluated and ranked in an ascending order in terms of their channel magnitudes utilizing only the currently positioned PAs, i.e.,

$$P_k^{(n)} = \left\| \bar{\mathbf{g}}_{BT_k}^{(n)}(\bar{\mathbf{x}}^{(n)}) \mathbf{H}(\bar{\mathbf{x}}^{(n)}) \right\|^2 \quad (14)$$

where $P_k^{(n)}$ is the evaluated channel gain for T_k while optimizing the PA locations at the n th waveguide, with $\bar{\mathbf{x}}^{(n)} \in \mathbb{R}^{1 \times ((n-1)M_t + G)}$ is a vector consisting of the optimized x -axis coordinates of the $(n-1)M_t + G$ PAs already positioned. Also,

$$\bar{\mathbf{g}}_{BT_k}^{(n)}(\bar{\mathbf{x}}^{(n)}) \triangleq \begin{bmatrix} \mathbf{g}_{B_1 T_k} \left(\left[\bar{\mathbf{x}}^{(n)} \right]_{1:M_t} \right), \dots, \\ \left[\mathbf{g}_{B_n T_k} \left(\left[\bar{\mathbf{x}}^{(n)} \right]_{(n-1)M_t+1:(n-1)M_t+G} \right) \right]_{1:G}, \\ \mathbf{0}_{1 \times ((N-n+1)M_t - G)} \end{bmatrix}, \quad (15)$$

with $\bar{\mathbf{g}}_{BT_k}^{(n)}(\bar{\mathbf{x}}^{(n)}) \in \mathbb{C}^{1 \times (NM_t)}$ being a zero-padded vector with $(n-1)M_t + G$ channel response elements of the positioned PAs with $[\mathbf{q}]_{a:b}$ denotes the portion of a vector \mathbf{q} between the indices a and b . Then, the K targets are sorted by their channel magnitudes, i.e., $P_{i_K}^{(n)} \geq \dots \geq P_{i_1}^{(n)}$, with i_k defining the target's index with the k th lowest channel magnitude. Afterwards, the remaining $M_t - G$ PAs in the n th waveguide are set in the current order of increasing channel magnitude of the K targets, i.e., starting from the target with the weakest channel magnitude (T_{i_1}). A PA is aligned with a target as follows: $x_{n,G+k} = x_{T_{i_k}}$, $k = 1, \dots, K$, assuming $|x_{T_{i_k}} - x_{T_{i_{k-1}}}| \geq \Delta x, \forall k \geq 2$. Note that in the case when $K > M_t - G$, a proportion of $K - M_t + G$ targets with the highest channel magnitude will not benefit from the optimized antenna placement according to their locations, as the proposed scheme focuses on enhancing the channel magnitude of the $M_t - G$ targets with the lowest channel magnitude. On the other hand, observe that when $K < M_t - G$ and $M_t - G \neq qK (q \in \mathbb{N}^*)$, some targets can have more than one PA aligned to its x -axis coordinate per the above-mentioned placement rule, where after placing the first K PAs out of the $M_t - G$ remaining ones, the considered scheme starts over again from T_{i_1} until completing positioning all the n th waveguide's PAs. In this case, it can be noted that co-locating two or more antennas at $x_{T_{i_k}}$ violates (13f). Therefore, in this scenario, the proposed scheme first checks when placing the $(m+G)$ th PA, if any of the already-positioned PAs is close to $x_{T_{i_{(m+G-1) \bmod K + 1}}}$ by less than Δx . If the latter condition is satisfied, the scheme performs a line search over the waveguide to find the location minimizing the distance to the current target in consideration, i.e., $T_{i_{(m+G-1) \bmod K + 1}}$ while fulfilling (13f) with already-positioned PAs in the same waveguide, i.e.,

$$x_{n,m+G} = \min_x \left(|x - x_{T_{i_{(m+G-1) \bmod K + 1}}}| \right), m = 1, \dots, M_t - G$$

$$\text{s.t. : } |x - x_{n,p}| \geq \Delta x (\forall p < m + G) \ \& \ x \in [x_0, x_{\max}]. \quad (16)$$

The aforementioned process is performed identically for the remaining waveguides.

C. Beamforming and AN Optimization

For an optimized PA positions vector $\mathbf{x}^{(\text{opt})}$ using the proposed scheme in the previous subsection, the optimization of $\{\mathbf{V}_g\}_{g=1}^G, \mathbf{W}$ is carried out by dropping \mathbf{x} from the control variables of (13). Observe that $\mathcal{P}1$ is challenging to optimize due to (i) the complex form of the objective function, i.e., max-min fairness problem, (ii) the non-convex SC expression in (13b) in terms of $\{\mathbf{V}_g\}_{g=1}^G, \mathbf{W}$, and the non-convex rank-

one constraint in (13c). To overcome this hurdle, the following alternative representation is considered

$$\mathcal{P}2 : \max_{\{\mathbf{V}_g\}_{g=1}^G, \mathbf{W}, \theta} \rho \quad (17a)$$

$$\text{s.t. (C1) : } \gamma_{U_g}^{(g)} \left(\{\mathbf{V}_g\}_{g=1}^G, \mathbf{W}, \mathbf{x}^{(\text{opt})} \right) \geq \gamma_{U,\text{lb}}, \forall g \quad (17b)$$

$$\text{(C2) : } \gamma_{T_k}^{(g)} \left(\{\mathbf{V}_g\}_{g=1}^G, \mathbf{W}, \mathbf{x}^{(\text{opt})} \right) \leq \gamma_{E,\text{ub}}, \forall g, k \quad (17c)$$

$$\text{(C3) : } \mathcal{Q}_s^{(k)} \left(\mathbf{R}_s, \mathbf{x}^{(\text{opt})} \right) \geq \rho \quad (17d)$$

$$(13c) - (13g) \quad (17e)$$

In (17), the SC constraint in (13b) was replaced by C1 and C2 in (17b) and (17c). The latter constraints can equivalently maintain a target minimal SC of the network by imposing a maximal received SINR at each malicious target $\gamma_{E,\text{ub}}$ while preserving a minimal SINR $\gamma_{U,\text{lb}}$ for each user for reliable signal decoding. Note from (7), (17b) and (17c) that C1 and C2 of (17) are convex. In addition, θ is involved as a slack variable to tackle the complex objective function form in (13). Herein, ρ is linked with the sensing illumination power of each target via C3 in (17d), which aims at maximizing the per-target illumination power. By relaxing the rank-one constraint in (13c), $\mathcal{P}2$ becomes a convex semidefinite program, which can be solved by any convex optimization tool, e.g., CVX. Then, an eigenvalue decomposition-based approach is used to transform $\{\mathbf{V}_g\}_{g=1}^G$ into rank-1 solutions by expressing them in terms of their principal eigenvectors [13].

IV. NUMERICAL RESULTS

This section presents numerical examples through which the performance of the proposed scheme is evaluated. Table I indicates the values of the various system parameters used in the simulations. The wavelength is linked to carrier frequency f_c as $\lambda = c/f_c$, where c is the speed of light in the vacuum. Furthermore, it is considered that all nodes and targets are positioned at the ground level, i.e., $z_{U_g} = z_{T_k} = 0, \forall t, k$. For the set of users and targets, the various nodes are distributed equidistantly over their respective angular and radius intervals given in Table I, where $d_{O\Lambda}$ is the distance from the origin ($x_O = 0, y_O = 0$) to Λ . In addition, $\varphi_{O\Lambda}$ denotes the azimuth relative angle of node Λ with respect to the origin O .

TABLE I: System Parameters Values

Parameter	Value/Interval	Parameter	Value/Interval
f_c	15 GHz	$G^{(B_n, m)}$	30 dB
$G^{(\Lambda)}$	10 dBi	d_{OU_g}	[40, 50] m
d_{OT_k}	[20, 40] m	φ_{OU_g}	[-50, -40]°
φ_{OT_k}	30°	y_n	15 + 5n m
$z_n (\forall n)$	10 m	σ_Λ^2	-110 dB
G	2	K	3
N	8	M_t	6
P_{\max}	20 dB	$\gamma_{E,\text{ub}}$	3 dB
x_0	0 m	x_{\max}	60 m

In Fig. 2, the proposed scheme's performance in terms of the illumination power is shown versus $\gamma_{U,\text{lb}}$ and compared against a baseline equidistant PAs positioning [14]. The latter approach positions the set of M_t PAs along each waveguide equidistantly with the first and last PAs at x_0 and x_{\max} , respectively. Observe that the proposed PAs positioning approach

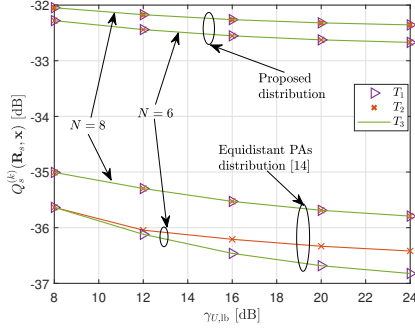


Fig. 2: Illumination power of the proposed scheme vs. $\gamma_{U,lb}$ compared with an equidistant PAs deployment [14].

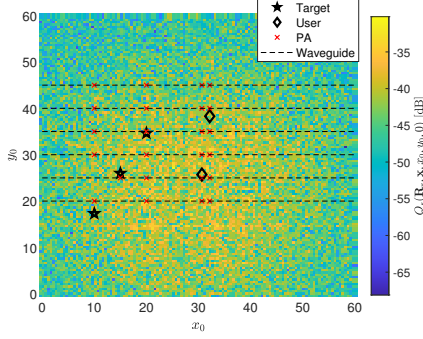


Fig. 3: Illumination power pattern over the considered communication and sensing area, along with the optimized PAs positions.

yields a higher target illumination power compared to the aforementioned baseline scheme, where 4-dB sensing gain is observed at $\gamma_{U,lb} = 24$ dB with $N = 6$ compared to the baseline scheme. Observe that per the proposed algorithm, only $M_t = G = 2$ PAs from each waveguide are positioned close to the corresponding users, whereas the remaining $M_t - G = 6$ PAs, representing a higher proportion, are placed in such a way to enhance the channel condition of the sensed targets. Also, observe the slight illumination power increase by increasing the network secrecy requirement in terms of $\gamma_{U,lb}$, showing an existing secrecy-sensing trade-off. In Fig. 3, the illumination power pattern over the considered geographical area is shown, evaluated using (12) with $N = 6$ and $M_t = 4$. The obtained results indicate a relatively large spot in the center of the area with scattered points of high illumination power. The sensed targets and users are positioned in relatively highly-illuminated positions, with $Q_s^{(1)} = Q_s^{(2)} = -39$ dB while $Q_s^{(3)} = -41.5$ dB.

In Fig. 4, the proposed scheme's sensing power is presented and compared against the baseline secure ISAC scheme in [13]. The latter consists of a dual-functional radar communication BS with a ULA of half-wavelength-spaced antennas, whereas the scheme aims at minimizing the total transmit power subject to the secrecy constraints in (17c) and (17d) and to a sensing constraint. The latter is defined by a maximal sidelobe-to-mainlobe ratio, chosen to -20 dB in our evaluation. For the sake of fairness, UL transmission is not considered in the baseline scheme, and P_{\max} for the proposed framework is set as the optimized power by the benchmark one. Also, we set $\gamma_{E,ub} = -6$ dB and $N = 6$. Note that the proposed and baseline schemes yield an increasing sensing power with the increase of $\gamma_{U,lb}$. This is due to the fact that a higher $\gamma_{U,lb}$ requires an increased signal and AN power for

legitimate signal and AN beamforming, resulting in increased illumination power. Furthermore, the proposed approach yields a high sensing illumination power compared with the baseline scheme, exceeding 30 dB.

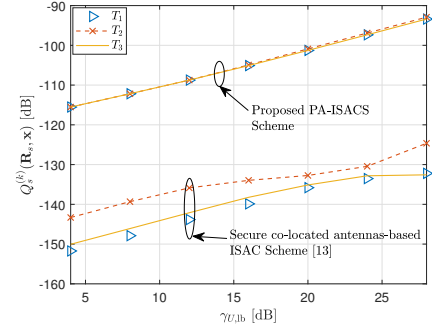


Fig. 4: Illumination power of the proposed scheme compared with the secure ISAC scheme of [13].

V. CONCLUSIONS

In this letter, we analyzed a robust and secure PA-ISAC system. The proposed approach invoked pinching beamforming to securely beamsteer information signals to various DL users in the presence of malicious targets, while maximizing the sensing signal power for the latter. A novel algorithm for obtaining suboptimal PA positions was proposed. Those locations were used to design optimal beamforming and AN covariance matrices, using semidefinite programming methods. The obtained results showed a notable enhancement in terms of sensing illumination power compared to the baseline secure ISAC scheme with traditional half-wavelength-spaced ULA.

REFERENCES

- [1] B. Liao *et al.*, "Power allocation for massive MIMO-ISAC systems," *IEEE Trans. Wireless Commun.*, vol. 23, no. 10, pp. 14 232–14 248, 2024.
- [2] E. Björnson *et al.*, "Massive MIMO: ten myths and one critical question," *IEEE Commun. Mag.*, vol. 54, no. 2, pp. 114–123, 2016.
- [3] A. Fukuda *et al.*, "Pinching antenna: Using a dielectric waveguide as an antenna," *NTT DOCOMO Technical J.*, vol. 23, no. 3, p. 5–12, 2022.
- [4] Z. Ding *et al.*, "Flexible-antenna systems: A pinching-antenna perspective," 2024. [Online]. Available: <https://arxiv.org/abs/2412.02376>
- [5] Z. Wang *et al.*, "Modeling and beamforming optimization for pinching-antenna systems," 2025. [Online]. Available: <https://arxiv.org/abs/2502.05917>
- [6] Y. Xu *et al.*, "Rate maximization for downlink pinching-antenna systems," 2025. [Online]. Available: <https://arxiv.org/abs/2502.12629>
- [7] A. Bereyhi *et al.*, "Downlink beamforming with pinching-antenna assisted MIMO systems," 2025. [Online]. Available: <https://arxiv.org/abs/2502.01590>
- [8] S. Tegos *et al.*, "Minimum data rate maximization for uplink pinching-antenna systems," *IEEE Wireless Commun. Lett.*, pp. 1–1, 2025.
- [9] P. P. Papanikolaou *et al.*, "Secrecy rate maximization with artificial noise for pinching-antenna systems," 2025. [Online]. Available: <https://arxiv.org/abs/2504.10656>
- [10] Z. Ding, "Pinching-antenna assisted ISAC: A CRLB perspective," 2025. [Online]. Available: <https://arxiv.org/abs/2504.05792>
- [11] W. Mao *et al.*, "Multi-waveguide pinching antennas for ISAC," 2025. [Online]. Available: <https://arxiv.org/abs/2505.24307>
- [12] Z. Zhang *et al.*, "Integrated sensing and communications for pinching-antenna systems (PASS)," 2025. [Online]. Available: <https://arxiv.org/abs/2504.07709>
- [13] A. Bazzi and M. Chafii, "Secure full duplex integrated sensing and communications," *IEEE Trans. Inf. Forensics Security*, vol. 19, pp. 2082–2097, 2024.
- [14] C. Ouyang *et al.*, "Array gain for pinching-antenna systems (pass)," *IEEE Commun. Lett.*, vol. 29, no. 6, pp. 1471–1475, 2025.